METEOROLOGICAL APPLICATIONS
Meteorol. Appl. **25**: 376–383 (2018)
Published online 11 December 2017 in Wiley Online Library
(wileyonlinelibrary.com) DOI: 10.1002/met.1705

Influence of moisture source and sink regions on northeast monsoon rainfall

P. Suneetha,[a]* P. Latha,[b] S. Ramalingeswara Rao[a] and O. S. R. U. Bhanu Kumar[a]

[a] *Department of Meteorology and Oceanography, Andhra University, Visakhapatnam, India*
[b] *Dr. V. S. Krishna Government Degree College, Visakhapatnam, India*

ABSTRACT: The northeast monsoon (NEM) over south India plays a vital role in producing light and moderate rainfall events during October through December. Excess NEM rainfall is mainly due to the intensified tropical cyclones and easterly waves from the Pacific east–west troughs over the Bay of Bengal. The main heat source and sink regions of this monsoon season are the western Pacific high and the Siberian high, respectively. Relative variations in the areal extent and intensity of these source and sink regions influence the NEM season by excess or deficient rainfall. Hence, the aim of the present study was to observe the impact of the Siberian high and the western Pacific high on the NEM rainfall in excess and deficient years. For this purpose, dynamic and thermodynamic parameters, the zonal and meridional winds, the velocity potential, the sea surface temperature and the relative humidity of the National Centers for Environmental Prediction and the National Center for Atmospheric Research (NCEP/NCAR) reanalysis data were used for the period 1951–2014. Analysis of these variables revealed the importance of the source and sink regions for the enhancement/reduction of NEM rainfall during excess/deficient years.

KEY WORDS monsoon; climate change impacts; extreme rainfall; hazards;

Received 8 November 2016; Revised 14 March 2017; Accepted 8 May 2017

1. Introduction

The south Indian winter/northeast monsoon (NEM) rainfall during October through December is less understandable than the summer/southwest monsoon over the Indian subcontinent. The NEM season is associated with dry monsoon winds, which blow from the continent over the Bay of Bengal and the Indian Ocean. The major heating centre of the Asian summer monsoon shifts southeastward from its usual location in south Asia to the maritime continent and the equatorial western Pacific during the NEM season and the following changes occur. Generally, in September the intensity of the summer monsoon circulation steadily decreases and by October the area is in its transition to the winter monsoon pattern over south India. Next, in November, the heat low that had been over Pakistan and northern India is replaced by a weak anticyclone, and the re-establishment of the near-equatorial trough close to 10°N heralds the establishment of the NEM over south India (Krishnamurti, 1973). The longitudinal alignment of the equatorial heat source region and the strong subtropical baroclinic zone gives rise to strong mid-latitude tropical interaction; these are distinctive features of the NEM season (Chang and Lau, 1980, 1982). Under the influence of an upper circulation a trough of low pressure forms and it extends from the Lakshadweep area to the east central Arabian Sea. This results in the formation of a dumb-bell shaped pressure field in the east–west direction and yields good monsoon rainfall over Tamilnadu and Kerala, especially in the onset of the NEM.

Over Asia, a huge and shallow thermal anticyclone called the Siberian high forms because of intense cooling of the land during the northern hemisphere winter (Hastenrath, 1985). Generally its pressure varies between 1026 and 1032 hPa. Murkami (1979) recognizes the cold surface high over Siberia as a source region of cold air outburst and considers the mountain barrier of the Himalayas as a factor for cold surges to reach west to about 90°E. This penetration of cold surges into the equatorial rain is seen as part of a regional scale of mean meridional Hadley circulation, with rising motion in the domain of the heaviest rainfall in the Malaysia–Indonesia area and subsidence over Siberia. Chang *et al.* (2006) underline the role of cold air surges emanating from the Siberian high in enhancing convection in the equatorial belt and thus contributing to the NEM heat engine. The Siberian maritime high has been used as an indicator for the intensity of the NEM rainfall (Jhun and Lee, 2004). Similarly the western Pacific high (WPH), the heat source region of the NEM, tends to be stronger in summer than in winter (Huang and Wu, 1989; Ding, 1994). The WPH is strong in the northern summer compared to the northern winter. This is because in winter the sea surface temperature (SST) difference is 3 °C but in summer the difference increases to as much as 6 °C. Murtugudde *et al.* (2003) described how the northern Pacific Ocean occupies maximum sea level pressure due to a seasonal exchange of mass between the Indian subcontinent and the ocean. In addition to the strong synoptic scale activities, the highest cyclonic activity also coincided over the western Pacific (Holland, 1984; McBride, 1995). More vigorous activity in one sector is apt to create subsidence in another and helps to suppress activity as the largest scales tend to be emphasized in the tropics (Webster, 1972). Land–ocean differential heating is also another driving force which leads to release of latent heat associated with intense convection from the western Pacific region (moisture source) and a strong cold dome residing to the northeast of the Siberian high is the heat sink.

Global warming in the recent decades refers to a rise in land and ocean temperatures that leads to changes in circulation, rainfall

* Correspondence: P. Suneetha, Department of Meteorology and Oceanography, Andhra University, Waltair, Visakhapatnam-530003, India. E-mail: sunitha.pmet@gmail.com

© 2017 Royal Meteorological Society

and pressure patterns. The abnormal warming of the equatorial waters of the central and eastern Pacific has often been associated with failure of the southwest monsoon (Bhalme and Mooley, 1980; Bhalme *et al.*, 1986; Bhanu Kumar and Ramalingeswara Rao, 2009; Bhanu Kumar *et al.*, 2011). However, the very same phenomenon appears to have just the opposite effect on the NEM, leading to more bountiful rain (Jayanthi and Govindhachari, 1999; Bhanu Kumar *et al.*, 2004, 2007). Kumar *et al.* (2007) examined the relationship between the El Niño–Southern Oscillation (ENSO) and the NEM rainfall for the period 1901–2000 and observed that strengthening of the easterly wind flow brings more moisture to the subcontinent and increases the NEM rainfall during an El Niño year. Moreover, the NEM rainfall during El Niño years after 1976 had on average become considerably more copious than during the period from 1950 to 1976. The NEM rains occur in spells of about 3–4 days duration (De and Mukhopadhyay, 1999). The NEM is confined to the southern peninsular region and brings about 11% of annual rainfall to India (Yadav, 2012). Yadav (2012) studied the ENSO influence on the Indian NEM in recent decades. During El Niño years the subsidence anomaly over the warm-pool region of Indonesia was much stronger in recent decades compared with earlier decades. Intensified tropical cyclones and storms strike southern peninsular India leading to flood years of the NEM. From the above information, an attempt is made in the present study to understand the influence of both the Siberian high (40–60°N; 70–120°E) and the WPH (10–50°N; 110–180°E) on NEM rainfall through different dynamic and thermodynamic variables and related changes in the moisture source and sink regions in the recent global warming period.

2. Data and methodology

The Indian Institute of Tropical Meteorology (IITM), Pune, subdivisional rainfall data (Pathasarathy *et al.*, 1994) are used for seven meteorological subdivisions of south India, namely Coastal Andhra Pradesh, Rayaleaseema, Tamilnadu, North Interior Karnataka, South Interior Karnataka, Coastal Karnatakara and Kerala (Figure 1), during October through December for 1951–2013. Adapted from the technique of Pathasarathy *et al.* (1994), Figure 2 reveals that there are six deficient years (1959, 1971, 1974, 1988, 1989 and 2000) and eight excess rainfall years (1956, 1966, 1977, 1987, 1993, 1994, 2005 and 2010).

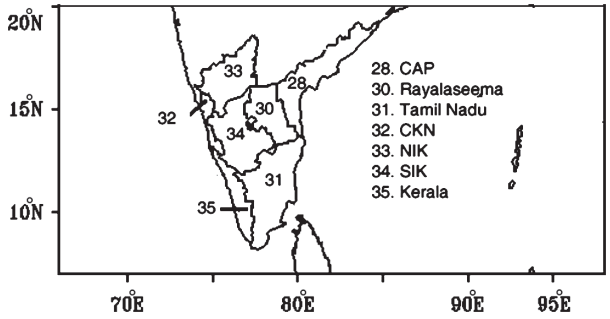


Figure 1. Meteorological subdivisions of the study.

Table 1. Number of normal rainy days (~2.5 mm day^{-1}) in the excess and deficient years.

Deficient years	No. of rainy days	Excess years	No. of rainy days
1959	28	1956	41
1971	30	1966	42
1974	25	1977	49
1988	10	1987	50
1989	17	1993	45
2000	30	1994	41
		2005	40
		2010	42

The numbers of NEM rainfall days are also quantified by using high resolution India Meteorological Department daily gridded rainfall data (1° × 1°) for 1951–2007 (Rajeevan *et al.*, 2005). An amount of rainfall greater than 2.5 mm day^{-1} is considered as a rainfall day in the present study; rainfall days during the excess and deficient years are shown in Table 1. The highest rainfall days are observed in 1987, while the lowest are in 1988. Mean monthly National Centers for Environmental Prediction/National Center for Atmospheric Research (NCEP/NCAR) reanalysis datasets (Kalnay *et al.*, 1996) were used to study air temperature, sea level pressure, zonal and meridional wind and relative humidity for the domain 5–80 ° N, 60–180°E for the period of 63 years (1951–2013). The National Oceanic and Atmospheric Administration (NOAA) optimum interpolated SST data were also retrieved to assess the impact of El Niño on NEM source/sink

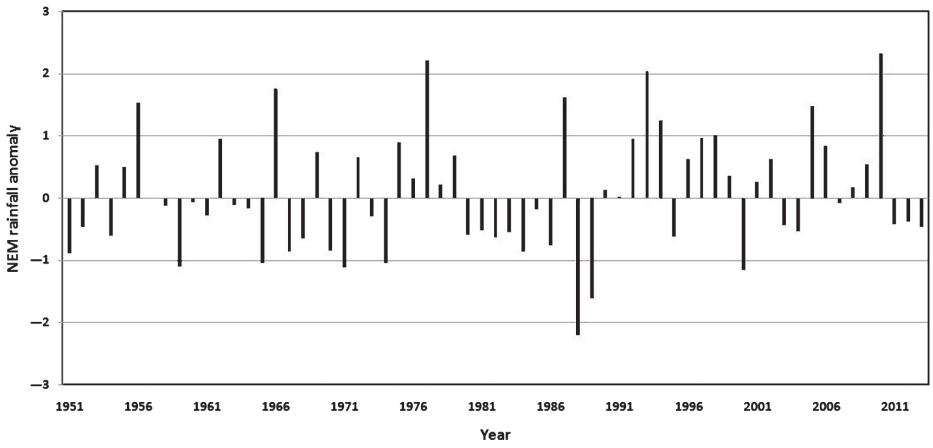


Figure 2. The Indian Institute of Tropical Meteorology subdivisional rainfall for the northeast monsoon (NEM) season with deficient (negative) values and excess (positive) values for the seven meteorological subdivisions for 1951–2013.

© 2017 Royal Meteorological Society

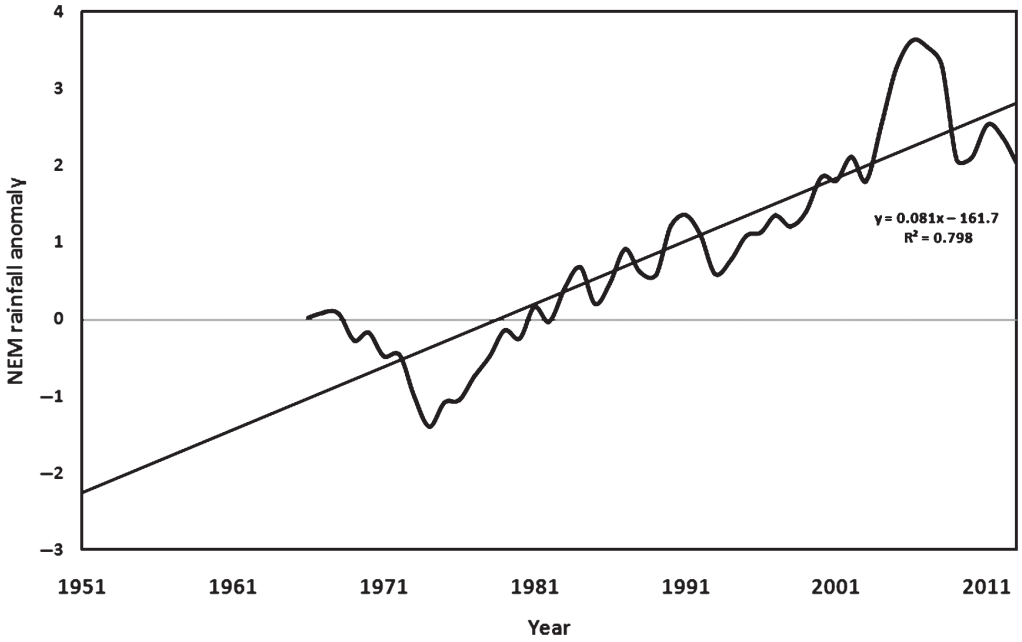


Figure 3. Cramer's test for the northeast monsoon (NEM) rainfall for the period 1951–2013.

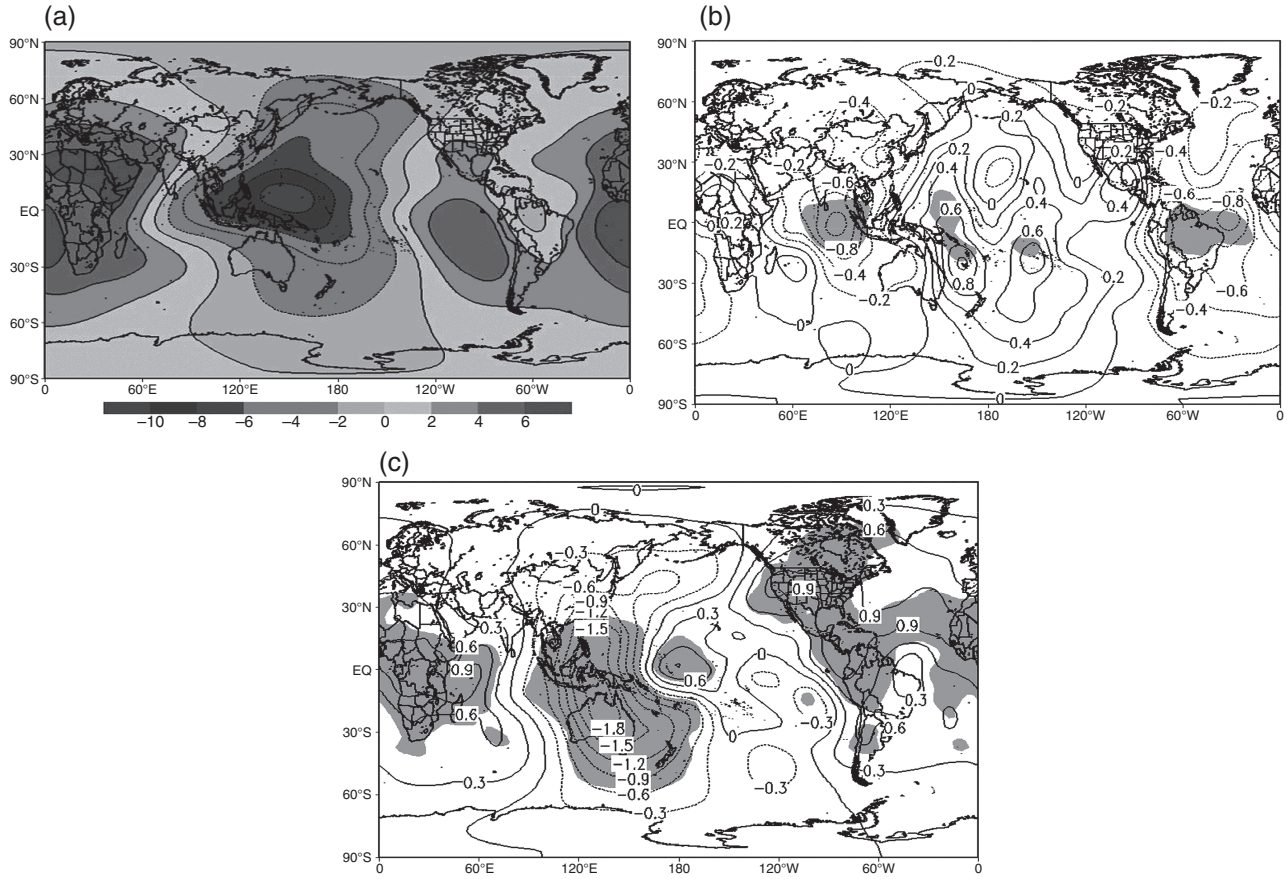


Figure 4. Anomalous characteristics of velocity potential ($\times 10^{-5}$ m^2 s^{-1}) at the 200 hPa level for the (a) northeast monsoon (NEM) climatology, (b) excess NEM years and (c) deficient NEM years. The grey shade indicates significance at the 95% level for Figures (b) and (c).

© 2017 Royal Meteorological Society

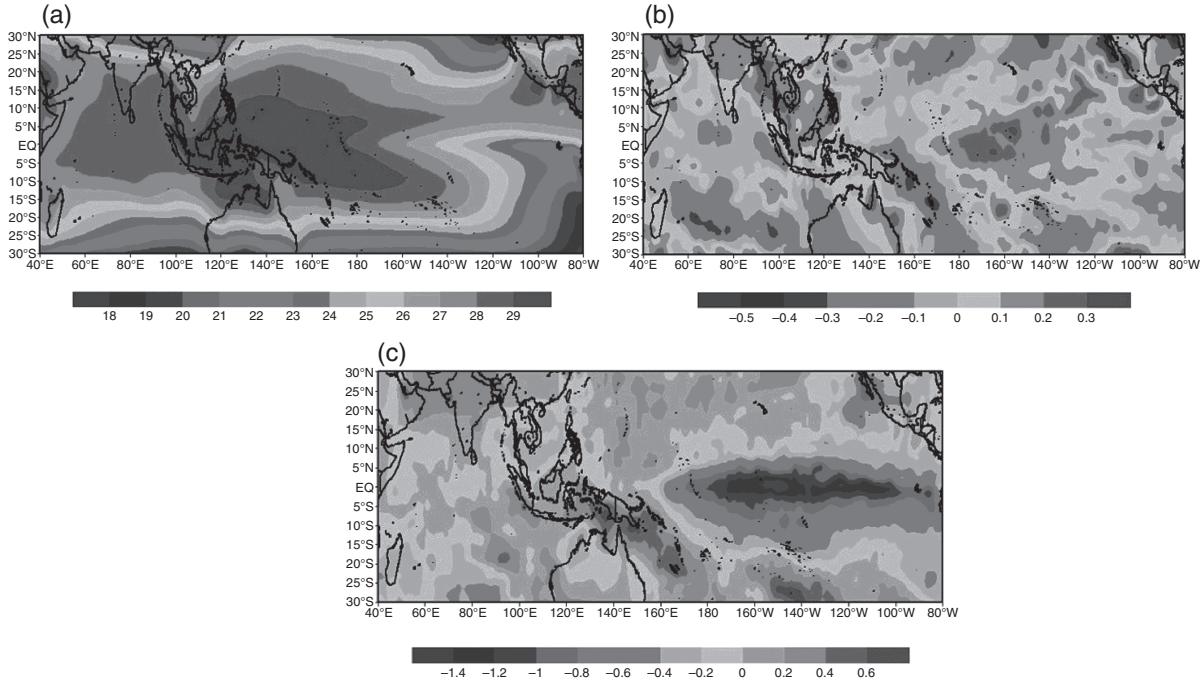


Figure 5. Anomaly of sea surface temperature (°C) for the (a) northeast monsoon (NEM) climatology, (b) excess and (c) deficient years during the NEM season for 1951–2013.

regions. Finally, velocity potential and moisture flux divergence were calculated for the study region.

2.1. Cramer's test

The climatic fluctuations of the NEM were studied by applying Cramer's test for 31 year running means. The computation procedure is as follows. The aim was to examine the stability of long term records in terms of a comparison between the overall mean of an entire record and the mean of a certain part of the record (WMO, 1966):

$$t_k = \sqrt{\left\{ \frac{n\,(N-2)}{N - n\left(1 + r_k^2\right)} \right\}} r_k$$

The statistic t_k is distributed as Student's t with $N-2$ degrees of freedom. This test may be repeated for any desired number and choice of sub-periods; here the sub-period was taken as 31 years (31 year climatic mean of the whole record). The time plot of the t value (plotted at the centre of the sub-period) gives a pictorial representation of the variability. Cramer's test also indicates that the NEM rainfall has been increasing since 1981 (Figure 3).

2.2. Statistical t test

The statistical significance of the composite anomaly obtained from the study period was evaluated using Student's t test for unequal variances (see Press *et al.*, 1992). The null hypothesis assumes that the composite excess/deficient year anomaly is not statistically significant. In order to test the null hypothesis, the test statistic given below was first computed, at each grid point:

$$t = \frac{\frac{1}{n_1}\sum_{i=1}^{n_1} a_i - \frac{1}{n_2}\sum_{i=1}^{n_2} c_i}{\left(\frac{\sigma_a^2}{n_1} + \frac{\sigma_c^2}{n_2}\right)^{1/2}}$$

where a_i are the excess/deficient anomalies for the excess and deficient years and c_i are the climatology (1951–2013) for each of the NEM seasons. Therefore, $n_1 = 186$ for climatology, $n_2 = 24$ for excess years and $n_3 = 18$ for deficient years. Here σ_a and σ_c correspond to the standard deviations of a_i and c_i, respectively. The degrees of freedom were calculated for unequal variance of excess and deficient years and were tested for 10% and 5% significance levels using the t tables.

2.3. Vertically integrated moisture flux divergence

The basic atmospheric water balance equation was formulated by Peixoto and Oort (1992) and can be written as:

$$\frac{\partial W}{\partial t} + \nabla \times Q = E - P$$

Here, E stands for evapotranspiration from the surface, P for precipitation and W for the vertically integrated water content *per* unit area; ∇ is the horizontal divergence operator and Q is the vertically integrated moisture flux (kg m^{-1} s^{-1}). The moisture flux divergence is calculated over the NEM domain using the above equation.

3. Results and discussion

Dynamic and thermodynamic variables such as zonal and meridional wind, air temperature and relative humidity play an important role for capturing moisture from heat source and sink regions to the NEM zone. Height–longitude Hovmöller diagrams indicate that changes in the thermodynamic variables lead to enhanced/reduced NEM rainfall over the study region.

3.1. Impact of velocity potential

In regions of deep convection the velocity potential is negative and consistent with the upper level air diverging away from updrafts. The anomaly of velocity potential for excess and

© 2017 Royal Meteorological Society

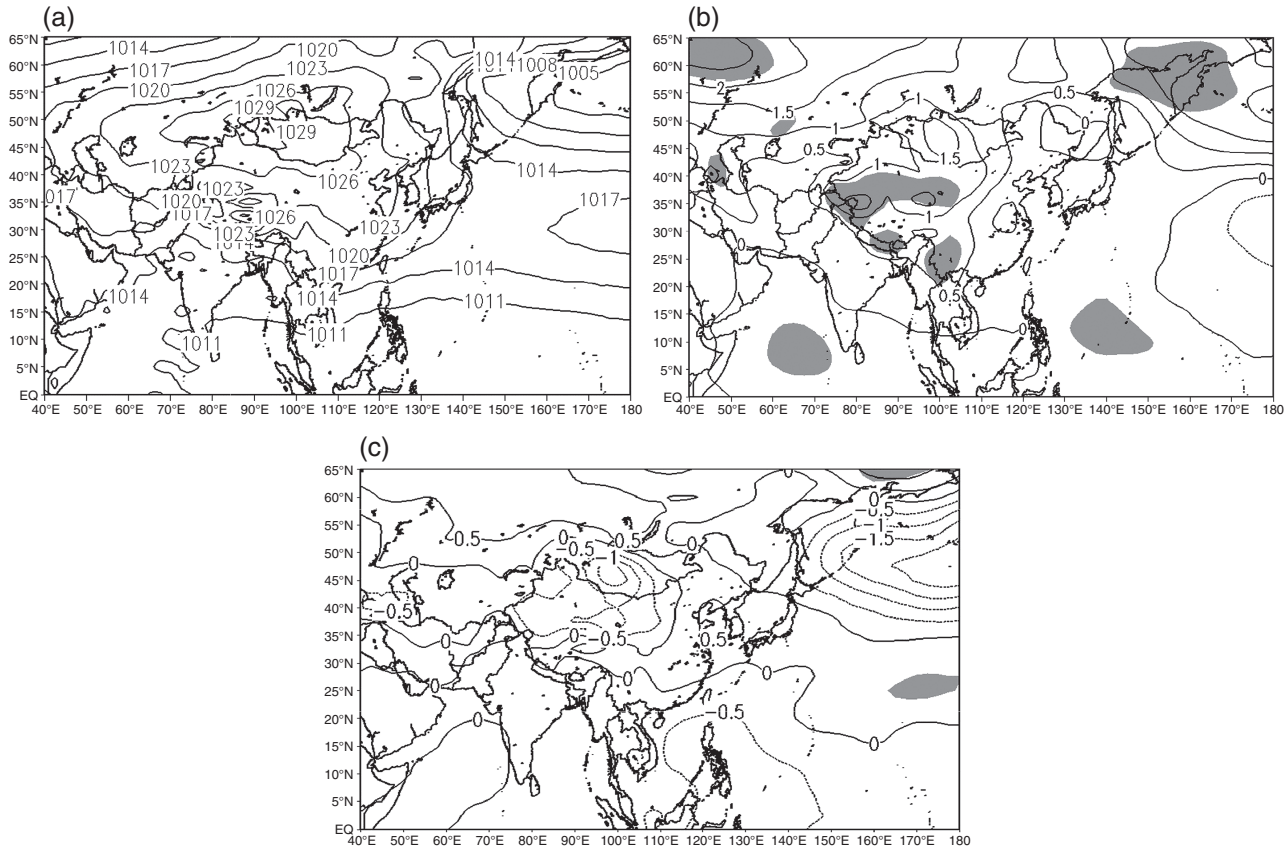


Figure 6. Same as Figure 5 but for sea level pressure (shading indicates the 90% significance level).

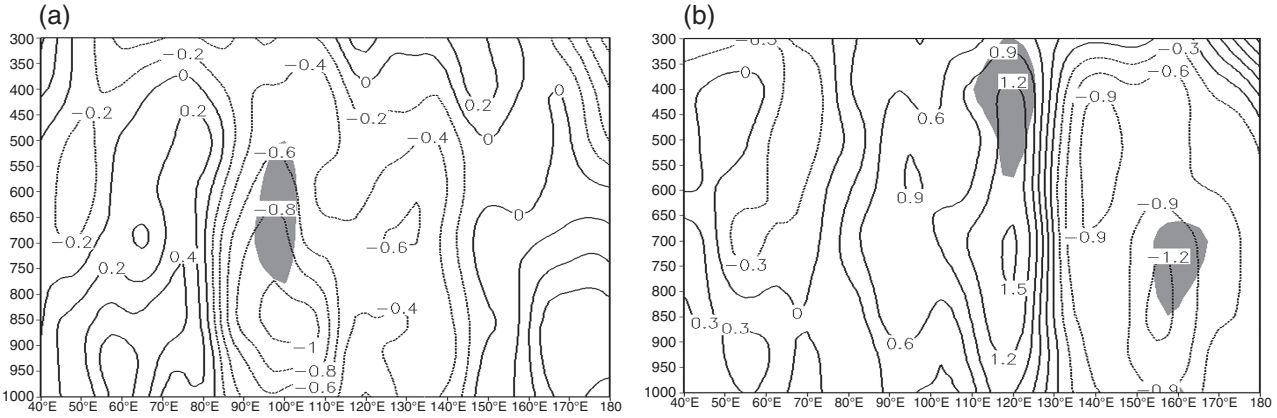


Figure 7. Hovmöller diagrams for the northeast monsoon region using zonal wind during the (a) northeast monsoon excess and (b) deficient rainfall years for 1951–2013 (shading indicates the 90% significance level).

deficient years during the NEM season for 1951–2013 is shown in Figures 4(a)–(c). The velocity potential varies in magnitude from −12 to 8 ($\times 10^{-5}$) for the above study period (Figure 4(a)). Deep convection is more prominent in the western Pacific region. During excess years, the anomaly of the velocity potential is mainly concentrated over the Bay of Bengal region (−0.4 to −0.6), while in deficient years it is mainly concentrated over Australia; it varies between −1.8 and −0.6 and is significant at the 95% level (Figure 4(b)). At 200 hPa, the divergence almost disappears over the south equatorial Pacific region.

In deficient years the central Pacific Ocean region showed that the velocity potential is about 0.9 compared to other regions of the study area (Figure 4(c)). The divergence region is mainly observed in the north–south direction over the Australia and Indonesia regions (−1.8 to −1.2). From the above analysis, it is observed that the moisture laden air transports more moisture towards the Bay of Bengal from the western Pacific Ocean through SST and ocean currents in excess years compared to deficient years. In this connection the WPH region provides more moisture through synoptic waves and regional circulations such as the northeast winds and easterly waves during the NEM season. Hence residuals of the WPH tropical cyclones and easterly waves provide a good amount of rainfall in the NEM season.

© 2017 Royal Meteorological Society

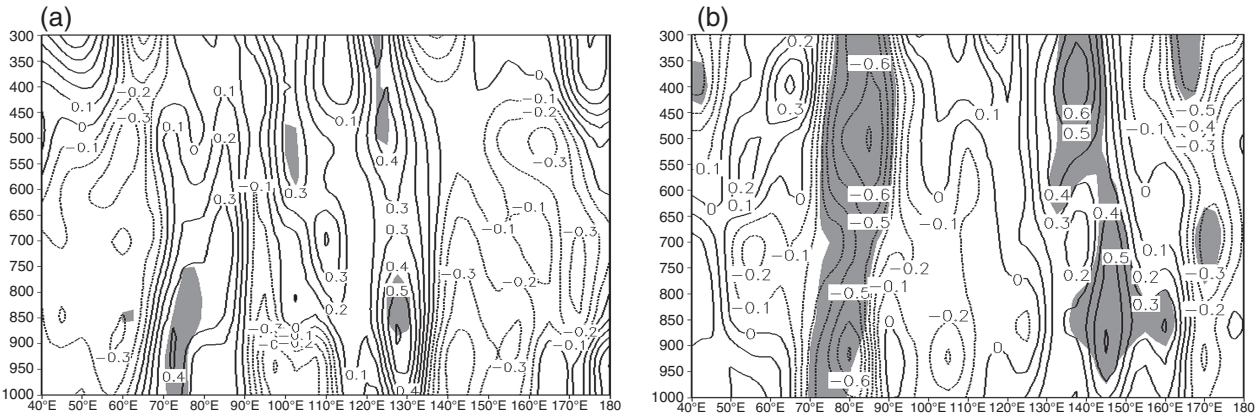


Figure 8. Same as Figure 7 but for meridional wind (shading indicates the 90% significance level).

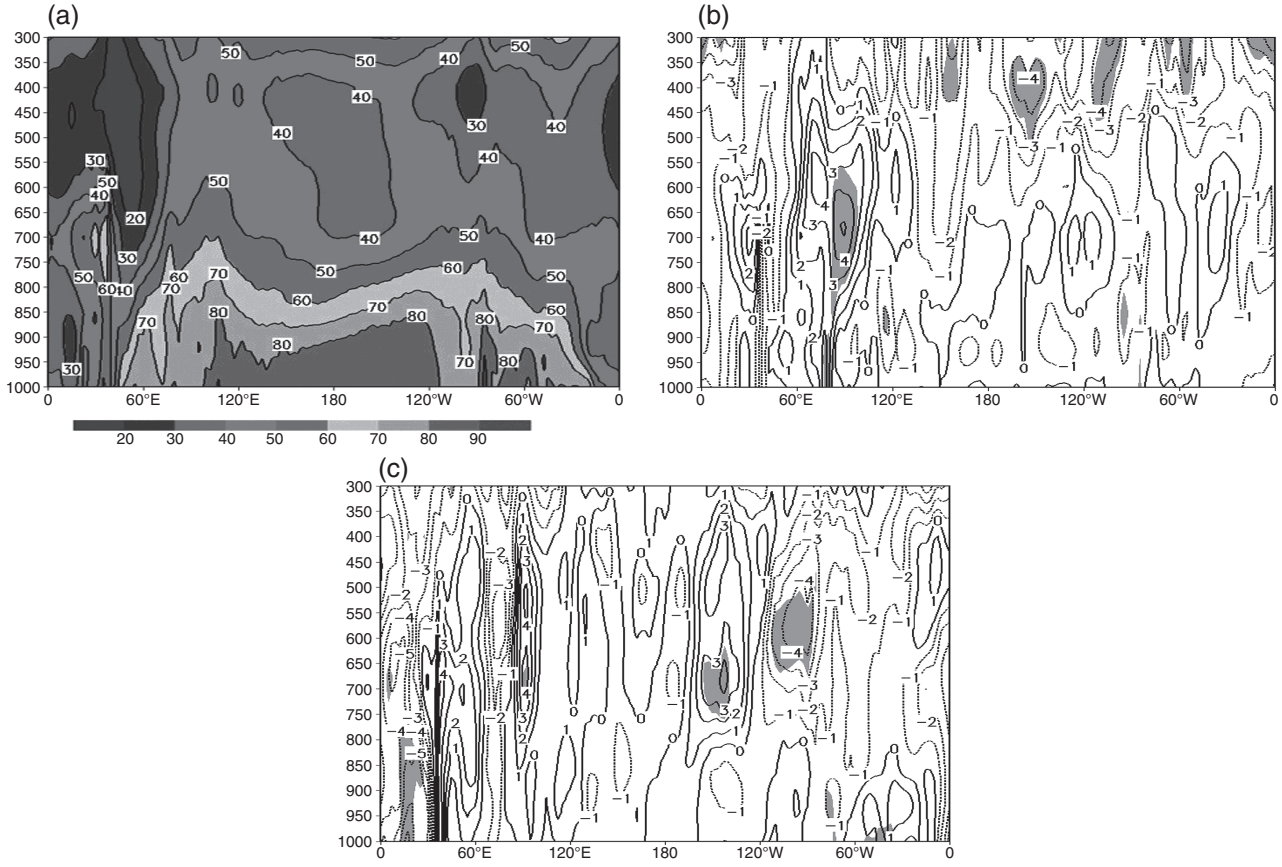


Figure 9. Same as Figure 6 but for relative humidity (grey shading of Figures (b) and (c) indicates the 95% significance level).

3.2. Influence of sea surface temperature

Anomalies of SST for excess and deficient years during the NEM season are shown in Figures 5(a)–(c). The analysis reveals that the composite of excess NEM rainfall years is associated with strong warming over the central Pacific Ocean, the Bay of Bengal and the Arabian Sea and cooling over the Indonesia region (Figure 5(b)). The recorded SST anomaly over warming regions is between 0.2 and 0.5 °C. The SST anomaly decreased during deficient years compared with excess years; the value is between −0.6 and −0.3 °C only and both the Bay of Bengal and the Arabian Sea are in the cooling phase (−0.1 °C) in Figure 5(c). Generally high temperatures over the Bay of Bengal provide moisture for getting more intense tropical cyclones, which leads to excess NEM rainfall. At the same time, over Indonesia and the western Pacific regions, the low temperatures lead to high pressure signatures for strong easterly winds over the Indian region (Gibies *et al.*, 2011). The reverse pattern appears in deficient years, i.e. warming is mainly concentrated over the central Indian Ocean region.

3.3. Sea level pressure changes

Sea level pressure changes of the NEM season were studied for 1951–2013 (Figures 6(a)–(c)). In the present study, it was observed that the climatological mean sea level pressure over the

© 2017 Royal Meteorological Society

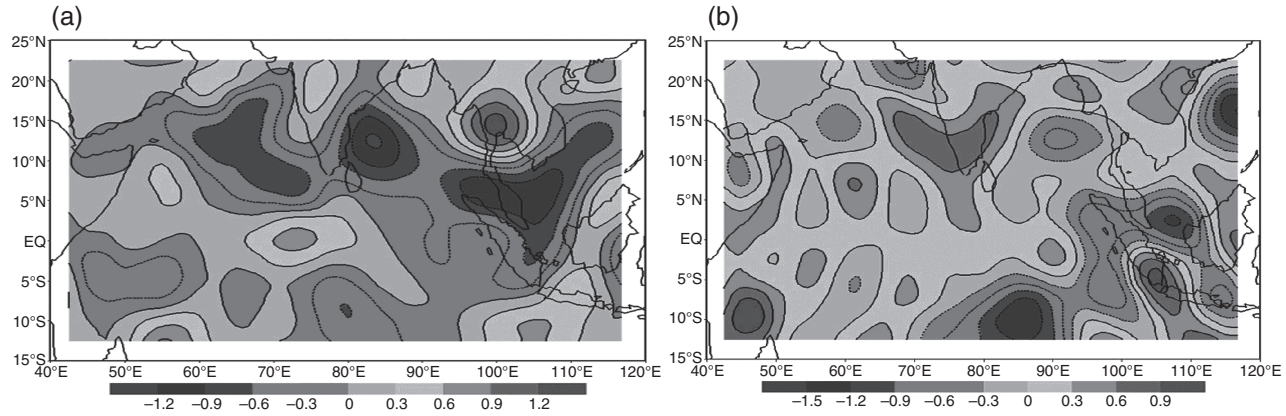


Figure 10. Moisture flux divergence (10^{-5} kg m^{-2} s^{-1}) due to anomalous wind in the (a) excess and (b) deficient northeast monsoon rainfall years.

Siberian high is 1029 hPa and for the NEM zone (south India) is only 1011 hPa (Figure 6(a)). Later the study was extended for eight excess and six deficient years. In the deficient years, the anomaly sea level pressure over the Siberian high was around 1.0 hPa only (Figure 6(c)), while it increased to about 1.0−1.5 hPa in excess years; these results are statistically significant at the 90% level (Figure 6(b)). Hence, there is a clear-cut demonstration that the anomaly of sea level pressure over the Siberian high region increases more in excess than in deficient years. This could be the reason for the strength in the northeasterly winds from the Siberian cold surges that leads to an increase in NEM rainfall activity.

3.4. Zonal wind aberrations

The height−longitude cross-section of zonal wind over the NEM season during excess years revealed that the WPH region is covered by an easterly wind regime with a maximum core in the mid-tropospheric levels with a magnitude of 1.4 m s^{-1} between 110°E and 180°E. The westerly zonal wind prevailed at lower levels (0.6−0.8 m s^{-1}) over the Arabian Sea region; these results are significant at the 90% level and are shaded in Figure 7(a). In deficient years, the zonal wind anomaly shows a westerly wind belt only with a magnitude of 1−1.5 m s^{-1} over the NEM zone (Figure 7(b)). In deficient years, the grey shaded zone indicates that the zonal wind is significant at the 95% level. From this it is observed that there are strong predominant easterlies at lower levels over the western Pacific which will lead to moisture in the Bay of Bengal in excess years. However, in deficient years, weak easterlies prevail at lower levels and lead to poor moisture over the NEM region.

3.5. Meridional wind

In deficient years, the strength of the easterlies extends up to 850 hPa only (Figure 8(b)). In excess years, the easterlies dominate up to 400 hPa (Figure 8(a)). The grey shaded zone indicates the 95% significance level. The meridional wind shows a direct Hadley cell over India during the NEM season. This further confirms that excess rainfall years are mainly constituted by strong easterlies in contrast to deficient years.

3.6. Relative humidity

Figures 9(a)−(c) represent the vertical cross-section of climatology and composite anomalies of relative humidity for excess and deficient years (centred at 11°N) for the study period. The longitude−height cross-sections show that saturation occurs at a middle level (700−200 hPa level) over the NEM region (80°E−110°E) during excess years. Strong relative humidity (>2 hPa) from the western Pacific region at lower levels and enhanced convection over the NEM region at the middle level are observed during excess years (Figure 9(b)). These results are positively significant at the 95% level. In deficient years the saturation is absent over the NEM region (Figure 9(c)).

3.7. Moisture flux divergence over the NEM region

From the analysis, it is evident that most of the moisture flux divergence during excess NEM rainfall years is situated over southern India (Figure 10(a)). The strength of the moisture flux divergence is mostly concentrated over the Bay of Bengal with a magnitude of -1.5×10^{-5} kg m^{-2} s^{-1}. During deficient years the moisture flux divergence is totally absent and is towards the southern Indian Ocean (Figure 10(b)).

4. Conclusions

In this study the standardized anomaly of rainfall indicates eight excess and six deficient years over the study period. The time series of the northeast monsoon (NEM) rainfall from Cramer's test indicates that there is an increasing trend from 1981 which supports the enhancement of rainfall during recent decades. The rainfall days also resemble the deficient and excess monsoon years. The results from the velocity potential, sea surface temperatures, sea level pressure and moisture flux divergence support that the heat source and sink regions are influencing the NEM rainfall activity in the excess/deficient years. Later, thermodynamic variables explain the northeasterly strength is very much greater at lower levels than at upper levels. Hence, this study highlights the quantitative and qualitative influence of heat source and sink regions on the NEM rainfall during excess and deficient years.

Acknowledgements

The authors are very grateful to the India Meteorological Department, New Delhi, and IITM, Pune, for providing the rainfall data. Special thanks to the NCEP/NCAR reanalysis team and the NOAA for data. The second author wishes to thank the University Grants Commission, New Delhi, for financial assistance through the Faculty Development Program to complete

© 2017 Royal Meteorological Society

this paper. The authors sincerely thank both of the anonymous reviewers, whose comments and critiques improved the quality of the paper.

References

Bhalme HN, Jadhav SK, Mooley DA, Ramana Murthy BV. 1986. Forecasting of monsoon performance over India. *Int. J. Climatol.* **6**(4): 347–354.

Bhalme HN, Mooley DA. 1980. Large scale droughts/floods and monsoon circulation. *Mon. Weather Rev.* **108**: 1197–1211.

Bhanu Kumar OSRU, Naidu CV, Ramalingeswara Rao S. 2004. Influence of Southern Oscillation and SSTs over Nino-3.4 region on the winter monsoon rainfall over coastal Andhra Pradesh. *Proc. Indian. Acad. Sci. (Earth Planet. Sci.)* **113**(3): 313–319.

Bhanu Kumar OSRU, Ramalingeswara Rao S, Muni Krishna K. 2007. Predictability of winter monsoon rainfall over south India using tropical sea surface temperatures. *Asia Pac. J. Atmos. Sci.* **43**(4): 449–456.

Bhanu Kumar OSRU, Ramalingeswara Rao S. 2009. Impact of global warming on life style of Indian farmers in the ensuing monsoon seasons. *International Conference on Climate Change and Impact on Life Style*, 13–14 November 2009, NGRI, Hyderabad.

Bhanu Kumar OSRU, Suneetha P, Ramalingeswara Rao S. 2011. Impact of rising sea surface temperatures on frequency of tropical storms and their relationships over north Indian Ocean. *Can. J. Pure Appl. Sci.* **5**(3): 1675–1683.

Chang CP, Lau KM. 1980. Northerly cold surges and near-equatorial disturbances over the winter MONEX area during December 1974. Part II: planetary-scale aspects. *Mon. Weather Rev.* **108**: 298–312.

Chang CP, Lau KM. 1982. Short-term planetary scale interaction over the tropics and the mid- latitudes. Part 1: contrast between active and inactive period. *Mon. Weather Rev.* **110**: 933–946.

Chang CP, Wang Z, Hendon H. 2006. The Asian winter monsoon. *The Asian Monsoon*, Wang B (ed). Springer Press: Chichester; 89–127.

De US, Mukhopadhyay RK. 1999. The effect of ENSO/anti ENSO on northeast monsoon rainfall. *Mausam* **50**: 343–354.

Ding YH. 1994. *Monsoon Over China*. Kluwer Academic Publishers: Dordrecht; 432.

Gibies G, Chalotte BV, Ruchity RD. 2011. Interannual variation of northeast monsoon rainfall over Southern Peninsular India. *Indian J. Geo-Mar. Sci.* **40**(1): 98–104.

Hastenrath S. 1985. *Climate and Circulation of the Tropics*. Vol. 8, Springer Netherlands. https://doi.org/10.1007/978-94-009-5388-8.

Holland GJ. 1984. On the climatology and structure of tropical cyclones in the Australian/Southwest Pacific region, I: data and tropical storms. *Aust. Met. Mag.* **32**: 1–16.

Huang RH, Wu YF. 1989. The influence of ENSO on the summer climate change in China and its mechanisms. *Adv. Atmos. Sci*. **6**: 21–32. https://doi.org/10.1007/BF02656915.

Jayanthi N, Govindachari S. 1999. El-Niño and northeast monsoon rainfall over Tamil Nadu. *Mausam* **50**: 217–218.

Jhun JG, Lee EJ. 2004. A new East Asian Winter Monsoon index and associated characteristics of the winter monsoon. *J. Climate* **17**: 711–725.

Kalnay E, Kanamitsu M, Kistler R, Collins W, Deaven D, Gandin L, *et al.* 1996. The NCEP/NCAR 40-year reanalysis project. *Bull. Am. Meteorol. Soc.* **77**: 437–471.

Krishnamurti TN. 1973. Tibetan high and upper tropospheric tropical circulation during northern summer. *Bull. Am. Meteorol. Soc.* **54**: 1234–1249.

Kumar P, Kumar KR, Rajeevan M, Sahai AK. 2007. On the recent strengthening of the relationship between ENSO and northeast monsoon rainfall over south-Asia. *Climate Dynam.* **28**: 649–660.

McBride JL. 1995. Tropical cyclone formation. Global perspectives on tropical cyclones, WMO/TD-No. 693. Tropical cyclone program report number 38, WMO: Geneva, Switzerland; 63–105.

Murkami M. 1979. Large-scale aspects of deep convective activity over the GATE area. *Mon. Weather Rev.* **107**: 994–1013.

Murtugudde R, Busalacchi AJ, McCreary JP. 2003. Comment on dipoles, temperature gradients, and tropical climate anomalies. *Bull. Am. Meteorol. Soc.* **84**: 1422–1423.

Pathasarathy B, Munot AA, Kothawale DR. 1994. All India monthly and seasonal rainfall series: 1871–1993. *Theor. Appl. Climatol*. **49**: 217–224.

Peixoto JP, Oort AH. 1992. *Physics of Climate*. Springer: Berlin.

Press WH, Teukolsky SA, Vetterling WT, Flannery BP. 1992. *Numerical Recipes in C: The Art of Scientific Computing*, Second Edition. Cambridge University Press: New York.

Rajeevan M, Bhate J, Kale JD, Lal B. 2005. Development of a high resolution daily gridded rainfall data for the Indian region. IMD Met Monograph No: Climatology 22/2005, 27. (Available from National Climate Centre, IMD Pune. ncc@imdpune.gov.in).

Yadav RK. 2012. Emerging role of Indian Ocean on Indian northeast monsoon. *Climate Dynam.* **41**: 105–116.

Webster PJ. 1972. Response of the tropical atmosphere to local, steady forcing. *Mon. Weather Rev.* **100**: 518–541.

© 2017 Royal Meteorological Society